Ferromagnetism in Malonato-Bridged Copper(II) Complexes. Synthesis, Crystal Structures, and Magnetic Properties of $\{[Cu(H_2O)_3][Cu(mal)_2(H_2O)]\}_n$ and $\{[Cu(H_2O)_4]_2[Cu(mal)_2(H_2O)]\}[Cu(mal)_2(H_2O)_2]\{[Cu(H_2O)_4][Cu(mal)_2(H_2O)_2]\}$ (H_2mal = malonic Acid)

Catalina Ruiz-Pérez,*[1a] Joaquín Sanchiz,[1b] María Hernández Molina,[1a] Francesc Lloret,*[1c] and Miguel Julve[1c]

Grupo de Rayos X del Departamento de Física Fundamental II, Universidad de La Laguna, Avda AstrofísicoFrancisco Sánchez s/n, 38204 La Laguna, Tenerife, Spain, Departamento de Química Inorgánica, Universidad de la Laguna, 38204 La Laguna, Tenerife, Spain, and Departament de Química Inorgànica, Facultat de Química de la Universitat de València, Dr. Moliner 50, 46100 Bujassot, València, Spain

Received July 9, 1999

Three malonato-bridged copper(II) complexes of the formulas $\{[Cu(H_2O)_3][Cu(C_3H_2O_4)_2(H_2O)]\}_n$ (**1**), $\{[Cu(H_2O)_4]_2[Cu(C_3H_2O_4)_2(H_2O)]\}[Cu(C_3H_2O_4)_2(H_2O)_2]\{[Cu(H_2O)_4][Cu(C_3H_2O_4)_2(H_2O)_2]\}$ (**2**), and $[Cu(H_2O)_4][Cu(C_3H_2O_4)_2(H_2O)_2]$ (**3**) ($C_3H_2O_4$ = malonate dianion) have been prepared, and the structures of the two former have been solved by X-ray diffraction methods. The structure of compound **3** was already known. Complex **1** crystallizes in the orthorhombic space group *Pcab*, $Z = 8$, with unit cell parameters of $a = 10.339(1)$ Å, $b = 13.222(2)$ Å, and $c = 17.394(4)$ Å. Complex **2** crystallizes in the monoclinic space group $P2/c$, $Z = 4$, with unit cell parameters of $a = 21.100(4)$ Å, $b = 21.088(4)$ Å, $c = 14.007(2)$ Å, and $\beta = 115.93(2)°$. Complex **1** is a chain compound with a regular alternation of aquabis(malonato)copper(II) and triaquacopper(II) units developing along the *z* axis. The aquabis(malonato)copper(II) unit acts as a bridging ligand through two slightly different *trans*-carboxylato groups exhibiting an *anti*−*syn* coordination mode. The four carboxylate oxygens, in the basal plane, and the one water molecule, in the apical position, describe a distorted square pyramid around Cu1, whereas the same metal surroundings are observed around Cu2 but with three water molecules and one carboxylate oxygen building the equatorial plane and a carboxylate oxygen from another malonato filling the apical site. Complex **2** is made up of discrete mono-, di-, and trinuclear copper(II) complexes of the formulas $[Cu(C_3H_2O_4)_2(H_2O)_2]^{2-}$, $\{[Cu(H_2O)_4][Cu(C_3H_2O_4)_2(H_2O)_2]\}$, and $\{[Cu(H_2O)_4]_2[Cu(C_3H_2O_4)_2(H_2O)]\}^{2+}$, respectively, which coexist in a single crystal. The copper environment in the mononuclear unit is that of an elongated octahedron with four carboxylate oxygens building the equatorial plane and two water molecules assuming the axial positions. The neutral dinuclear unit contains two types of copper atoms, one that is six-coordinated, as in the mononuclear entity, and another that is distorted square pyramidal with four water molecules building the basal plane and a carboxylate oxygen in the apical position. The overall structure of this dinuclear entity is nearly identical to that of compound **3**. Finally, the cationic trimer consists of an aquabis(malonato)copper(II) complex that acts as a bismonodentate ligand through two *cis*-carboxylato groups (*anti*−*syn* coordination mode) toward two tetraaquacopper(II) terminal units. The environment of the copper atoms is distorted square pyramidal with four carboxylate oxygens (four water molecules) building the basal plane of the central (terminal) copper atom and a water molecule (a carboxylate oxygen) filling the axial position. The magnetic properties of **1**−**3** have been investigated in the temperature range 1.9−290 K. Overall, ferromagnetic behavior is observed in the three cases: two weak, alternating intrachain ferromagnetic interactions ($J = 3.0$ cm^{-1} and $\alpha J = 1.9$ cm^{-1} with $\hat{H} = -J\sum_i[\hat{S}_{2i}\cdot\hat{S}_{2i-1} + \alpha\hat{S}_{2i}\cdot\hat{S}_{2i+1}]$) occur in **1**, whereas the magnetic behavior of **2** is the sum of a magnetically isolated spin doublet and ferromagnetically coupled di- ($J_3 = 1.8$ cm^{-1} from the magnetic study of the model complex **3**) and trinuclear ($J = 1.2$ cm^{-1} with $\hat{H} = -J(\hat{S}_1\cdot\hat{S}_2 + \hat{S}_1\cdot\hat{S}_3)$ copper(II) units. The exchange pathway that accounts for the ferromagnetic coupling, through an *anti*−*syn* carboxylato bridge, is discussed in the light of the available magneto-structural data.

Introduction

Magneto-structural studies on polynuclear complexes, aimed at understanding the structural and chemical factors that govern the exchange coupling between paramagnetic centers through multiatom bridges, are of continuing interest in biology, chemistry, and physics.[1−6] The preparation of multifunctional, molecular-based materials that exhibit unusual magnetic, optical, and electrical properties is one of the issues of this fundamental research.[7,9]

The carboxylate group is one of the most widely used bridging ligands for designing polynuclear complexes with interesting

(1) (a) Departamento de Física Fundamental II de la Universidad de La Laguna. (b) Departamento de Química Inorgánica de la Universidad de La Laguna. (c) Departament de Química Inorgànica de la Universitat de València.

(2) *Magneto-Structural Correlations in Exchange Coupled Systems*; Willett, R. D., Gatteschi, D., Kahn, O., Eds.; NATO ASI Series C140; Reidel: Dordrecht, 1985.

(3) Kahn, O. *Struct. Bonding (Berlin)* **1987**, *68*, 89.

10.1021/ic9908165 CCC: $19.00
Published on Web 03/09/2000

Scheme 1

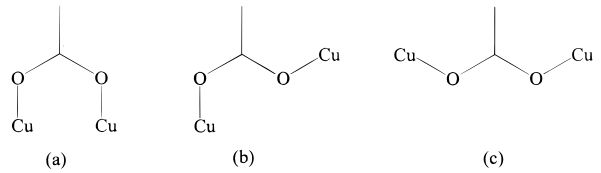

magnetic properties. Its versatility as a ligand is illustrated by the variety of its coordination modes when acting as a bridge,[10,11] the most common being the so-called *syn*−*syn*, *syn*−*anti*, and *anti*−*anti* modes (Scheme 1). Magnetic studies on structurally characterized carboxylato-bridged copper(II) complexes reveal that strong antiferromagnetic interactions (singlet−triplet energy gap ∼300 cm^{-1}) are mediated by the *anti*−*anti* bridging mode.[10,12] However, there are fewer weak ferro- and antiferromagnetic couplings which are observed in the two latter cases.[13−22] Within this context, a few reports have been devoted to the malonate-containing copper(II) complexes. (Malonate is the dianion of the propanedioic acid, hereafter denoted as mal.)[23−30] The versatility of malonate as a ligand is enhanced not only by the fact that it contains two carboxylate groups but also by the fact that they are located in the 1,3-positions. Consequently, malonate can simultaneously adopt chelating bidentate and different carboxylato-bridging coordination modes. Under this structural complexity, coupled magneto-structural studies are required to investigate the magnetic behavior of malonato complexes.

In the present work, we illustrate both the versatility of malonate as a ligand toward copper(II) and the importance of structural knowledge in magnetic studies. The synthesis, structural characterization, and magnetic investigation of the two new complexes of formulas $\{[Cu(H_2O)_3][Cu(mal)_2(H_2O)]\}_n$ (**1**) and $\{[Cu(H_2O)_4]_2[Cu(mal)_2(H_2O)]\}[Cu(mal)_2(H_2O)_2]$ $\{[Cu(H_2O)_4][Cu(mal)_2(H_2O)_2]\}$ (**2**) are herein reported. Complex **1** is an alternating copper(II) chain compound, whereas **2** is a very rare complex that is made up of mono-, di-, and trinuclear copper(II) units.

Experimental Section

Materials. Malonic acid, basic copper(II) carbonate $CuCO_3 \cdot Cu(OH)_2$, pyridine, and 4,4′-bipyridine were purchased from commercial sources and used as received. The dinuclear complex $[Cu(H_2O)_4][Cu(mal)_2(H_2O)_2]$ (**3**) was prepared as reported in the literature.[28] Elemental analyses (C, H) were performed on an EA 1108 CHNS−O microanalytical analyzer.

Synthesis of Compounds. $\{[Cu(H_2O)_3][Cu(mal)_2(H_2O)]\}_n$ **(1).** Basic copper(II) carbonate (0.221 g, 1 mmol) suspended in 15 mL of water was allowed to react with malonic acid (0.208 g, 2 mmol) at 50 °C to give a clear blue solution, which was allowed to reach room temperature. Next, pyridine (0.160 g, 2 mmol) mixed with 5 mL of water was added under stirring. The pH value of the final solution was 5.10. Flat, pale-blue crystals of **1** were separated from the mother liquor by slow evaporation at room temperature. The crystals were filtered off, washed with water and acetone, and dried on filter paper. The yield was 0.230 g (58%). Anal. Calcd for $C_6H_{12}O_{12}Cu_2$ (**1**): C, 17.86; H, 2.97. Found: C, 17.95; H, 3.10.

$\{[Cu(H_2O)_4]_2[Cu(mal)_2(H_2O)]\}[Cu(mal)_2(H_2O)_2]\{[Cu(H_2O)_4][Cu(mal)_2(H_2O)_2]\}$ **(2).** This compound was prepared by following an analogous procedure to that of **1** but replacing pyridine with 4,4′-bipyridine (1.25 mmol as the total amount). Turquoise-blue polyhedral crystals of **2** were grown by slow evaporation at room temperature. They were filtered off, washed with a small amount of cold water, and dried on filter paper. The yield was 0.402 g (92%). Anal. Calcd for $C_{18}H_{46}O_{41}Cu_6$ (**1**): C, 16.63; H, 3.54. Found: C, 16.71; H, 3.58.

Physical Techniques. IR spectra (450−4000 cm^{-1}) of compounds **1** and **2** were recorded on a Bruker IF S55 spectrophotometer with samples prepared as KBr pellets. Variable-temperature (1.9−290 K) magnetic susceptibilty measurements on polycrystalline samples of **1**−**3** were carried out with a Quantum Design SQUID operating at 100 G (T < 50 K) and 1000 G (over all of the temperature ranges). Diamagnetic corrections of the constituent atoms were estimated from Pascal's constant[31] as -160×10^{-6} (**1**), -545×10^{-6}(**2**), and -186×10^{-6} (**3**) $cm^3\ mol^{-1}$. Experimental susceptibilities were also corrected for the temperature-independent paramagnetism ($60 \times 10^{-6}\ cm^3\ mol^{-1}$ per Cu(II)) and the magnetization of the sample holder.

Crystallographic Data Collection and Structural Determination. Crystals having the dimensions 0.45 × 0.30 × 0.24 mm and 0.45 × 0.60 × 0.27 mm for **1** and **2**, respectively, were used for data collection on an Enraf-Nonius MACH3 four-circle diffractometer. The orientation matrix and lattice parameters were obtained by a least-squares refinement of the diffraction data of 25 reflections within the range $6° < \theta < 18°$.[32,33] Data were collected at 293(2) K using graphite-monochro-

(4) *Organic and Inorganic Low-Dimensional Crystalline Materials*; Delhaès, P., Drillon, M., Eds.; NATO ASI Series B168; Plenum: New York, 1987.
(5) *Molecular Magnetic Materials*; Gatteschi, D., Kahn, O., Miller, J., Eds.; NATO ASI Series E198; Kluwer: Dordrecht, 1991.
(6) Kahn, O. *Molecular Magnetism*; VCH: New York, 1993.
(7) *Molecular Magnetism: From Molecular Assemblies to the Devices*; Coronado, E., Delhaès, P., Gatteschi, D., Miller, J., Eds.; NATO ASI Series E321; Kluwer: Dordrecht, 1996.
(8) *Magnetism: A Supramolecular Function*; Kahn, O., Ed.; NATO ASI Series C484; Kluwer: Dordrecht, 1996.
(9) *Supramolecular Engineering of Synthetic Metallic Materials*; Veciana, J., Rovira, C., Amabilino, D. B., Eds.; NATO ASI Series C518; Kluwer: Dordrecht, 1999.
(10) (a) Deacon, G. B.; Phillips, R. J. *Coord. Chem. Rev.* **1980**, *33*, 227. (b) Melnik, M. *Coord. Chem. Rev.* **1981**, *36*, 1. (c) Kato, M.; Muto, Y. *Coord. Chem. Rev.* **1988**, *92*, 45.
(11) Oldham, C. In *Comprehensive Coordination Chemistry*; Wilkinson, G., Gillard, R. D., McCleverty, J. A., Eds.; Pergamon Press: Oxford, 1987; Vol. 2, p 435.
(12) (a) Bleaney, B.; Bowers, K. D. *Proc. R. Soc. London, Ser. A* **1952**, *214*, 451. (b) Figgis, B. N., Martin, R. L. *J. Chem. Soc.* **1956**, 3837. (c) Doedens, R. J. *Prog. Inorg. Chem.* **1976**, *21*, 209.
(13) Kolks, G.; Lippard, S. J.; Waszack, J. V. *J. Am. Chem. Soc.* **1980**, *102*, 4832.
(14) Corvan, P. J.; Estes, W. E.; Weller, R. R.; Hatfield, W. E. *Inorg. Chem.* **1980**, *19*, 1927.
(15) Caughlin, P. K.; Lippard, S. J. *J. Am. Chem. Soc.* **1984**, *106*, 2328.
(16) Carling, R. L.; Kopinga, K.; Kahn, O.; Verdaguer, M. *Inorg. Chem.* **1986**, *25*, 1786.
(17) Fuertes, A.; Miravitlles, C.; Escrivá, E.; Coronado, E.; Beltrán, D. *J. Chem. Soc., Dalton Trans.* **1986**, 1795.
(18) Towle, D. K.; Hoffmann, S. K.; Hatfield, W. E.; Singh, P.; Chaudhuri, P. *Inorg. Chem.* **1988**, *27*, 394.
(19) Levstein, P. R.; Calvo, R. *Inorg. Chem.* **1990**, *29*, 1581.
(20) Sapiña, F.; Escrivá, E.; Folgado, J. V.; Beltrán, A.; Beltrán, D.; Fuertes, A.; Drillon, M. *Inorg. Chem.* **1992**, *31*, 3851.
(21) (a) Colacio, E.; Costes, J. P.; Kivekäs, R.; Laurent, J. P.; Ruiz, J. *Inorg. Chem.* **1990**, *29*, 4240. (b) Colacio, E.; Domínguez-Vera, J. M.; Costes, J. P.; Kivekäs, R.; Laurent, J. P.; Ruiz, J.; Sundberg, M. *Inorg. Chem.* **1992**, *31*, 774. (c) Colacio, E.; Domínguez-Vera, J. M.; Kivekäs, R.; Moreno, J. M.; Romerosa, A.; Ruiz, J. *Inorg. Chim. Acta* **1993**, *212*, 115.
(22) Asai, O.; Kishita, M.; Kubo, M. *J. Phys. Chem.* **1959**, *63*, 96.
(23) Dubicki, L.; Harris, C. M., Kokot, E.; Martin, R. L. *Inorg. Chem.* **1966**, *5*, 93.
(24) Figgis, B. N.; Martin, D. J. *Inorg. Chem.* **1966**, *5*, 100.
(25) Britton, H. T. S.; Jarrett, E. D. *J. Chem. Soc.* **1935**, 168.
(26) Dimitrova, G. I.; Ablov, A. V.; Kiosse, G. A.; Popovich, G. A.; Malinovskii, T. I., Burshtein, I. F. *Dokl. Akad. Nauk SSSR* **1974**, *216*, 1055.
(27) Pajunen, A., Nasakkala, E. *Finn. Chem. Lett.* **1977**, 189.
(28) Chattopadhyay, D.; Chattopadhyay, S. K., Lowe, P. R.; Schwalke, C. H.; Mazumber, S. K.; Rana, A.; Ghosh, S. *J. Chem. Soc., Dalton Trans.* **1993**, 913.
(29) Suresh, E.; Bhadbhade, *Acta Crystallogr.* **1977**, *C53*, 193.
(30) Gil de Muro, I.; Mautner, F. A.; Insausti, M.; Lezama, L.; Arriortua, M. I.; Rojo, T. *Inorg. Chem.* **1998**, *37*, 3243.
(31) Earshaw, A. *Introduction to Magnetochemistry*; Academic Press: London, 1968.
(32) Enraf-Nonius, CAD-4 EXPRESS, Version 5.1/5.2; Enraf-Nonius: Delft, The Netherlands, 1994.

Table 1. Crystallographic Data for $\{[Cu(H_2O)_3][Cu(mal)_2(H_2O)]\}_n$ (**1**) and $\{[Cu(H_2O)_4]_2[Cu(mal)_2(H_2O)]\}[Cu(mal)_2(H_2O)_2]\{[Cu(H_2O)_4][Cu(mal)_2(H_2O)_2]\}$ (**2**)

compd	**1**	**2**
form	$C_6H_{12}O_{12}Cu_2$	$C_{18}H_{46}O_{41}Cu_6$
fw	403.1	1299.3
space grp	*P*cab	*C*2/*c*
a/Å	10.339(1)	21.100(4)
b/Å	13.222(2)	21.088(4)
c/Å	17.394(4)	14.007(2)
β/deg	90.0	115.93(2)
V/Å^3	2377.7(7)	5605(2)
Z	8	4
T (K)	293(2)	293(2)
ρ_{calcd} (g cm^{-3})	2.253	2.025
λ (Å)	0.71073	0.71073
μ(Mo Kα) (cm^{-1})	36.42	31.1
R^a	0.037	0.040
$R_w{}^b$	0.114	0.114

^{a} $R = \Sigma||F_o|-|F_c||/\Sigma|F_o|$. ^{b} $R_w = [\Sigma_w(|F_o|^2 - |F_c|^2)^2]/\Sigma_w|F_o|^2]^{1/2}$.

matized Mo Kα radiation ($\lambda = 0.710\ 73$ Å) and the ω-scan technique. A summary of the crystallographic data and structure refinement is given in Table 1. An examination of three standard reflections, monitored every 2 h, showed no sign of crystal deterioration. The index ranges of data collection were $-14 \le h \le 4$, $-18 \le k \le 7$, and $-24 \le l \le 0$ for **1** and $0 \le h \le 29$, $-29 \le k \le 8$, and $-19 \le l \le 17$ for **2**. Of the 3462 (**1**) and 8147 (**2**) measured independent reflections, in the θ range 2.50−30.0°, (**1**, **2**), 2765 (**1**), and 6302 (**2**) have $I > 2\sigma(I)$. All of the measured independent refletions were used in the analysis. The intensity data were corrected for Lorentz polarization and absorption.[34] The maximum and minimum trasmission factors were 0.923 and 0.564 for **1** and 0.978 and 0.496 for **2**.

The structures of **1** and **2** were solved by direct methods, followed by successive Fourier synthesis through SIR97.[35] All non-hydrogen atoms were refined anisotropically by full-matrix least-squares techniques on F^2 by using the SHELXL97[36] computational program. The hydrogen atoms of the malonate ligand were either found (**1**) or set in calculated positions (**2**) and isotropically refined as riding atoms. The remaing hydrogen atoms were neither found nor calculated. Full-matrix least-squares refinement was performed minimizing the function $\sum_w (|F_o|^2 - |F_c|^2)$ with $w = 1/[\sigma^2(F_o)^2 + mP^2 + nP]$ and $P = (F_o^2 + 2F_c^2)/3$ with $m = 0.064$ (**1**) and 0.0669 (**2**) and $n = 4.4143$ (**1**) and 14.6387 (**2**). The values of the discrepancy indices R (R_w), for all of the data, were 0.054 (0.122) for **1** and 0.057 (0.122) for **2**, whereas those listed in Table 1 correspond to the data with $I > 2\sigma(I)$. The final Fourier-difference map showed maximum and minimum height peaks of 0.72 and −0.83 e Å^{-3} for **1** and 0.84 and −0.74 e Å^{-3} for **2**. The largest and mean Δ/σ are 0.21 and 0.01 (**1**) and 0.01 and 0.001(**2**). The values of the number of reflections/number of variable parameters are 17.5 (**1**) and 20.5 (**2**). The values of the goodness-of-fit are 1.08 (**1**) and 1.09 (**2**). The analytical expressions of neutral scattering factors were used, and anomalous dispersion corrections were incorporated.[37] The final geometrical calculations and the graphical manipulations were carried out with PARST97[38] and PLATON[39] programs, respectively. Selected interatomic bond distances and angles for **1** and **2** are listed in Tables 2 and 3, respectively.

(33) A. L. Spek, *HELENA: Program for Data Reduction*; Utrecht University: The Netherlands, 1997.
(34) González-Platas, J.; Ruiz-Pérez, C. *NEWCORR: Program for Empirical Absorption Correction*; University of La Laguna: La Laguna, Spain, 1997.
(35) Altomare, A.; Burla, M. C.; Camalli, M.; Cascarano, G.; Giacovazzo, C.; Guagliardi, A.; Moliterni, A. G. G.; Polidori, G.; Spagna, R. SIR97: A New Tool for Crystal Structure Determination and Refinement. *J. Appl. Crystallogr.*, in press.
(36) Sheldrick, G. M. *SHELXL97: Program for the Refinement of Crystal Structures*; University of Göttingen: Göttingen, Germany, 1997.
(37) *International Tables for X-ray Crystallography*; Kynoch Press: Birmingham, 1974; Vol. 4, pp 55, 99, and 149.
(38) Nardelli, M. PARST95. *J. Appl. Crystallogr.* **1995**, *28*, 659.
(39) Spek, A. L. *Acta Crystallogr.* **1990**, *A46*, C-34.

Table 2. Selected Bond Lengths (Å) and Angles (deg) for Compound **1**[a,b]

Cu(1)−O(1)	1.930(2)	Cu(2)−O(7)	1.989(2)
Cu(1)−O(3)	1.933(2)	Cu(2)−O(2w)	1.925(3)
Cu(1)−O(5)	1.947(2)	Cu(2)−O(3w)	1.981(2)
Cu(1)−O(6)	1.934(2)	Cu(2)−O(4w)	1.957(2)
Cu(1)−O(1w)	2.454(2)	Cu(2)−O(2c)	2.185(2)
O(1)−Cu(1)−O(3)	92.7(1)	O(7)−Cu(2)−O(2w)	89.9(1)
O(1)−Cu(1)−O(5)	165.4(1)	O(7)−Cu(2)−O(3w)	161.2(1)
O(1)−Cu(1)−O(6)	87.4(1)	O(7)−Cu(2)−O(4w)	88.3(1)
O(1)−Cu(1)−O(1w)	95.8(1)	O(7)−Cu(2)−O(2a)	88.4(1)
O(3)−Cu(1)−O(5)	86.8(1)	O(2w)−Cu(2)−O(2c)	87.9(1)
O(3)−Cu(1)−O(6)	179.8(1)	O(3w)−Cu(2)−O(2w)	110.1(1)
O(3)−Cu(1)−O(1w)	89.9(1)	O(3w)−Cu(2)−O(2c)	87.8(1)
O(5)−Cu(1)−O(6)	93.0(1)	O(4w)−Cu(2)−O(2w)	178.1(1)
O(5)−Cu(1)−O(1w)	98.8(1)	O(4w)−Cu(2)−O(3w)	93.7(1)
O(6)−Cu(1)−O(1w)	90.2(1)	O(4w)−Cu(2)−O(2c)	92.7(1)

[a] Estimated standard deviations in the last significant digits are given in parentheses. [b] Symmetry code: (c) $-x$, $^1/_2 - y$, $^1/_2 + z$.

Table 3. Selected Bond Lengths (Å) and Angles (deg) for Compound **2**[a,b]

	mononuclear unit		
Cu(5)−O(13)	1.946(2)	Cu(5)−O(12w)	2.403(4)
Cu(5)−O(14)	1.941(2)		
O(13)−Cu(5)−O(13c)	88.9(1)	O(13)−Cu(5)−O(14c)	179.7(1)
O(13)−Cu(5)−O(14)	91.0(1)	O(14)−Cu(5)−O(14c)	89.0(1)
O(13)−Cu(5)−O(12w)	91.1(1)	O(14)−Cu(5)−O(12w)	89.3(1)
	dinuclear unit		
Cu(1)−O(1)	1.946(2)	Cu(2)−O(3w)	1.924(3)
Cu(1)−O(3)	1.944(2)	Cu(2)−O(4w)	1.920(2)
Cu(1)−O(5)	1.951(2)	Cu(2)−O(5w)	1.931(2)
Cu(1)−O(6)	1.945(2)	Cu(2)−O(6w)	1.927(3)
Cu(1)−O(1w)	2.404(3)	Cu(2)−O(7)	2.384(2)
Cu(1)−O(2w)	2.487(3)		
O(1)−Cu(1)−O(3)	91.8(1)	O(6)−Cu(1)−O(2w)	90.0(1)
O(1)−Cu(1)−O(5)	178.9(1)	O(1w)−Cu(1)−O(2w)	179.2(1)
O(1)−Cu(1)−O(6)	89.0(1)	O(7)−Cu(2)−O(3w)	91.9(1)
O(1)−Cu(1)−O(1w)	90.2(1)	O(7)−Cu(2)−O(4w)	90.6(1)
O(1)−Cu(1)−O(2w)	89.7(1)	O(7)−Cu(2)−O(5w)	97.0(1)
O(3)−Cu(1)−O(5)	88.4(1)	O(7)−Cu(2)−O(6w)	92.6(1)
O(3)−Cu(1)−O(6)	179.1(1)	O(3w)−Cu(2)−O(4w)	89.2(1)
O(3)−Cu(1)−O(1w)	91.1(1)	O(3w)−Cu(2)−O(5w)	89.2(1)
O(3)−Cu(1)−O(2w)	89.8(1)	O(3w)−Cu(2)−O(6w)	175.5(1)
O(5)−Cu(1)−O(6)	90.8(1)	O(4w)−Cu(2)−O(5w)	172.3(1)
O(5)−Cu(1)−O(1w)	88.7(1)	O(4w)−Cu(2)−O(6w)	90.9(1)
O(5)−Cu(1)−O(2w)	91.5(1)	O(5w)−Cu(2)−O(6w)	190.1(1)
O(6)−Cu(1)−O(1w)	89.2(1)		
	trinuclear unit		
Cu(3)−O(9)	1.938(4)	Cu(4)−O(8w)	1.915(2)
Cu(3)−O(10)	1.941(2)	Cu(4)−O(9w)	1.932(2)
Cu(3)−O(7w)	2.508(3)	Cu(4)−O(10w)	1.936(2)
		Cu(4)−O(11w)	1.932(2)
		Cu(4)−O(12)	2.381(3)
O(9)−Cu(3)−O(9a)	88.9(1)	O(12)−Cu(4)−O(8w)	92.3(1)
O(9)−Cu(3)−O(10)	91.7(1)	O(12)−Cu(4)−O(9w)	90.2(1)
O(9)−Cu(3)−O(10a)	179.4(1)	O(12)−Cu(4)−O(10w)	95.5(1)
O(9)−Cu(3)−O(7w)	90.2(1)	O(12)−Cu(4)−O(11w)	94.5(1)
O(10)−Cu(3)−O(10a)	87.8(1)	O(8w)−Cu(4)−O(9w)	177.3(1)
O(10)−Cu(3)−O(7w)	90.0(1)	O(8w)−Cu(4)−O(10w)	91.1(1)
O(10a)-Cu(3)−O(7w)	91.0(1)	O(8w)−Cu(4)−O(11w)	90.1(1)
		O(9w)−Cu(4)−O(10w)	89.7(1)
		O(9w)−Cu(4)−O(11w)	88.7(1)
		O(10w)−Cu(4)−O(11w)	169.9(1)

[a] Estimated standard deviations in the last significant digits are given in parentheses. [b] Symmetry code: (a) $1 - x$, y, $^{-1}/_2 - z$; (c) $-x$, y, $^{-1}/_2 - z$.

Results and Discussion

Description of the Structures. Compound 1. The structure of **1** consists of zigzag chains of copper(II) ions that exhibit a regular alternation of aquabis(malonato)copper(II) and triaquacopper(II) units, the former being linked to the latter as bismonodentate ligands though two *trans*-malonato oxygen atoms

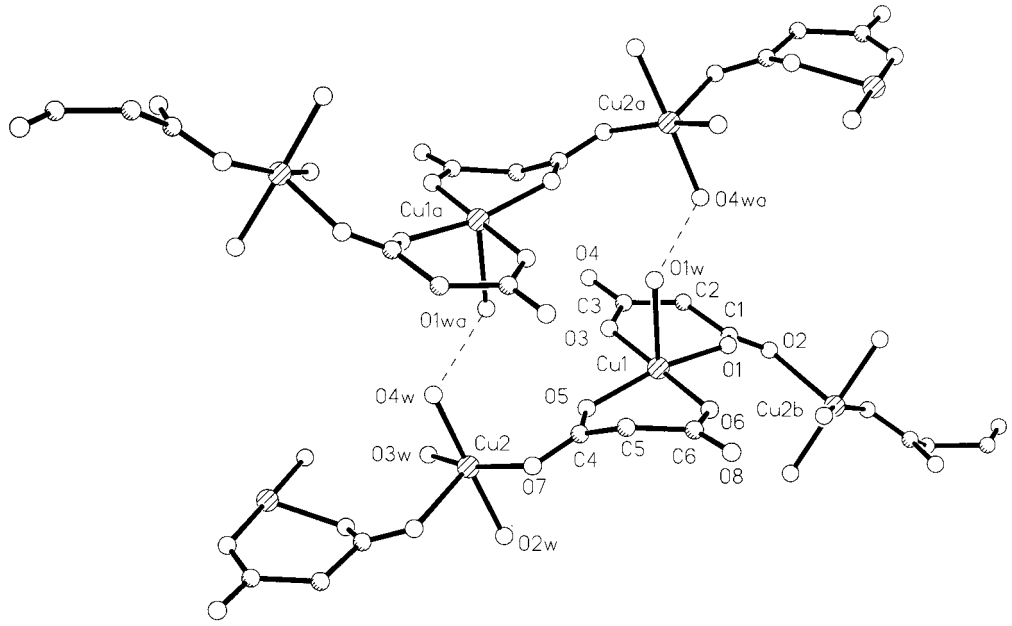

Figure 1. Perspective view of the asymmetric unit of **1** along with the atom numbering. The symmetry related unit of the adjacent chain is included to show the interchain hydrogen bonding interactions (broken lines). The thermal ellipsoids are drawn at the 30% probability level and the hydrogen atoms have been omitted for clarity.

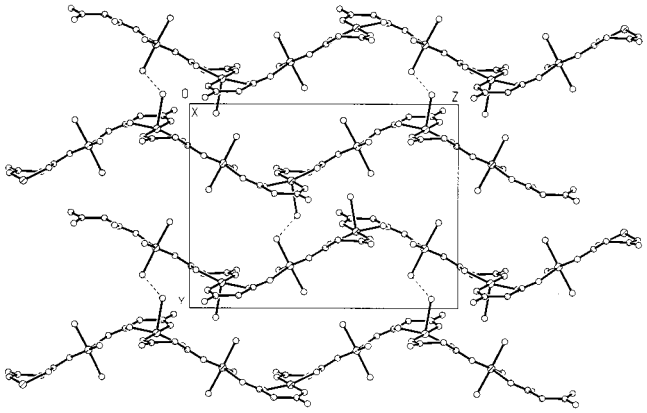

Figure 2. Projection of the structure of **1** down the *x* axis, showing its sheetlike nature.

(Figure 1). The chains run parallel to the *z* axis, and they are interconnected through hydrogen bonds involving the water molecule of the aquabis(malonato)copper(II) unit (O(1*w*)) and one of the coordinated water molecules (O(4*wa*)) of the triaquacopper(II) entity of the adjacent chain (2.816(3) Å for O(1*w*)···O(4*wa*); $a = -x, -y + 1, -z$). The formation of tetrameric copper(II) pairs through these hydrogen bonding interactions leads to a sheetlike polymeric structure that grows in the *yz* plane (Figure 2). Additional hydrogen bonds (O···O distances ranging from 2.534(4) to 2.911(4) Å), involving the remaining water molecules and the O(8), O(4), and O(2) carboxylate oxygens, contribute to stabilize the resulting three-dimensional network.

The two crystallographically independent copper(II) ions (Cu(1) and Cu(2)) have distorted square pyramidal surroundings. The four coplanar carboxylate oxygen atoms (O(1), O(3), O(5), and O(6)), which are coordinated to Cu(1) with practically identical oxygen to copper bond lengths (1.930(2)−1.947(2) Å), define the basal plane, whereas the apical position is occupied by a weakly coordinated water molecule (2.454(2) Å for Cu(1)−O(1w)). Cu(1) is shifted by 0.1243(4) Å from the basal plane toward O(1w). The average value of the copper to malonate oxygen bond distance lies within the range of similar bonds with carboxylate (1.92−2.16 Å).[40] The difference between the length of the axial and equatorial bonds (0.518 Å) is in excellent agreement with the $R_L - R_S$ value (0.51 Å) reported by Hathaway,[40a] R_L and R_S representing the lengths of the axial and equatorial copper to oxygen bonds, respectively. The angles subtended at Cu(1) by the chelating malonato groups are 92.7(1) and 93.0(1)°. The three water molecules O(2w), O(3w), and O(4w) and the carboxylate oxygen O(7) build the basal plane at Cu(2), whereas the other carboxylate oxygen, O(2c), occupies the axial position. The values of the O(7)-Cu(2)−O(3w) and O(3w)−Cu(2)−O(2w) bond angles (161.2(1) and 110.1(1)°, respectively) reflect the highly distorted square pyramidal surrounding at Cu(2). Cu(2) is shifted by 0.1972(4) Å from the mean basal plane toward the axial O(2c) atom. The calculated value of the τ factor[40b] for Cu(2) is 0.28, a value that indicates a significant distortion of the metal surroundings, from square pyramidal ($\tau = 0$) toward trigonal bipyramidal ($\tau = 1$).

Each malonate group simultaneously adopts bidentate (at Cu(1)) and monodentate (at Cu(2)) coordination modes and exhibits an envelop conformation in which only the methylene group is significantly shifted from the chelate ring plane. The average C−O bond distances and O−C−O bond angles are 1.256 Å and 122.5°, respectively. Two slightly different carboxylate bridges (O(1)C(1)O(2) and O(5)C(4)O(7)), that exhibit the *anti*−*syn* conformation, alternate regularly within each copper(II) chain. The bond angles at the bridging O(2) and O(7) atoms are 117.0(2) and 118.4(2)°, respectively. The values of the dihedral angle between the equatorial plane at Cu(1) and those of the O(1)C(1)O(2) and O(5)C(4)O(7) bridging carboxylates are 140.9(2) and 152.2(2)°. These values are far from the corresponding values between the equatorial plane at Cu(2) and the O(1*c*)C(2*c*)O(2*c*) and O(5)C(4)O(7) carboxylate planes, which are 47.6(2) and 90.4(2)°, respectively. The two intrachain copper−copper separations are 4.854(1) (Cu(1)···Cu(2)) and 4.640(1) Å (Cu(1)···Cu(2*b*); $b = -x, {}^1/_2 - y, -{}^1/_2 + z$), whereas

(40) (a) Hathaway, B. J. *Struct. Bonding (Berlin)* **1973**, *14*, 49. (b) Addison, A. W.; Rao, T. N.; Reedijk, J.; van Rijn, J.; Verschoor, G. C. *J. Chem. Soc., Dalton Trans.* **1984**, 1349.

Table 4. Hydrogen Bonding Interactions in the Crystal Structure of **2**

X···Y	X···Y/Å	symmetry operation generating Y	units linked
		monomer	
O(12w)···O(2)	2.808(4)	$-x+1/2, -y+1/2, -z$	monomer···dimer
O(12w)···O(7)	2.926(4)	$x, -y, z-1/2$	monomer···dimer
		dimer	
O(1w)···O(12)	2.981(4)	$x, -y, z+1/2$	dimer···trimer
O(1w)···O(16)	2.784(4)	$x, -y, z+1/2$	dimer···monomer
O(2w)···O(11)	2.775(4)	$-x+1/2, -y+1/2, -z$	dimer···trimer
O(2w)···O(15)	2.848(4)	$-x+1/2, -y+1/2, -z$	dimer···monomer
O(3w)···O(5)	2.691(3)	$-x, -y, -z$	dimer···dimer
O(3w)···O(11)	2.625(3)	$x-1/2, y-1/2, z$	dimer···trimer
O(4w)···O(7)	2.681(4)	$x-1/2, y-1/2, z$	dimer···dimer
O(4w)··O(14)	2.670(3)	$x-1/2, y-1/2, z$	dimer···monomer
O(5w)···O(4)	2.613(4)	$x, -y, z-1/2$	dimer···dimer
O(5w)···O(9)	2.721(3)	$x-1/2, y-1/2, z$	dimer···trimer
O(6w)···O(3)	2.684(4)	$x, -y, z-1/2$	dimer···dimer
O(6w)···O(16)	2.599(3)	$x, -y, z-1/2$	dimer···trimer
		trimer	
O(7w)···O(4)	2.868(4)	$-x+1/2, -y+1/2, -z$	trimer···dimer
O(7w)···O(8)	2.765(4)	$x, -y, z-1/2$	trimer···dimer
O(8w)···O(2)	2.598(4)	$-x+1, y, -z+1/2$	trimer···dimer
O(8w)···O(13)	2.652(4)	$-x+1/2, -y+1/2, -z$	trimer···monomer
O(9w)···O(8)	2.613(4)	$-x+1/2, -y+1/2, -z$	trimer···monomer
O(10w)···O(6)	2.699(4)	$-x+1/2, -y+1/2, -z$	trimer···dimer
O(10w)···O(15)	2.632(3)	$-x+1/2, -y+1/2, -z$	trimer···monomer
O(11w)···O(1)	2.696(3)	$-x+1, y, -z+1/2$	trimer···dimer

the shortest interchain copper−copper separations are 5.345(1) (Cu(1)···Cu(1*a*)) and 5.581(1) Å (Cu(1)···Cu(2*a*)).

Compound 2. The structure of complex **2** is made up of mono- (Figure 2a), di- (Figure 2b), and trinuclear (Figure 2c) copper(II) units of the formulas $[Cu(mal)_2(H_2O)_2]^{2-}$, $\{[Cu(H_2O)_4][Cu(mal)_2(H_2O)_2]\}$, and $\{[Cu(H_2O)_4]_2[Cu(mal)_2(H_2O)]\}^{2+}$, respectively, which are linked by electrostatic forces, van der Waals interactions, and an extensive network of hydrogen bonds involving the carboxylate groups and the water molecules (see Table 4 and Figure 4). In all of the hydrogen bonds, the water oxygens are the donor atoms, whereas the free or coordinated carboxylate oxygens act as acceptor atoms, with the O···O separations ranging from 2.598(4) to 2.981(4) Å. This is a very rare case, in which three copper(II) complexes of different nuclearity and containing the same ligand coexist in the same crystal. Previous examples in the chemistry of copper(II) were known but only two different entities were present in them.[41]

The coordination about Cu(5) in the mononuclear unit (Figure 3a) is elongated octahedral CuO_6 . Four carboxylate oxygens from two bidentate malonates build the equatorial plane, with copper to oxygen bonds nearly identical (1.946(2) and 1.941(2) Å for Cu(5)−O(13) and Cu(5)−O(14), respectively), whereas two water molecules occupy the axial sites (2.403(4) Å for Cu(5)−O(12w)). The values of the Cu−O(malonato) bonds agree with those previously reported for other malonato-containing copper(II) complexes.[26−30] All of the bond angles around Cu(5) are very close to the ideal ones. The trigonally distorted octahedral CuO_6 entity can be adequately described by two structural parameters, namely the degree of compression (s/h) and the angle of twisting (ϕ).[42] In $[Cu(mal)_2(H_2O)_2]^{2-}$, the values of these parameters are 1.36 and 53.97°, respectively, to be compared with 1.22 and 60° in a perfect octahedron. All of the bond lengths and angles of the malonato ligand are unexceptional. It adopts the same envelope conformation as most of its metal complexes. The value of the angle at C(11) deviates significantly from the tetrahedral (119.2(2)° for C(10)−C(11)−

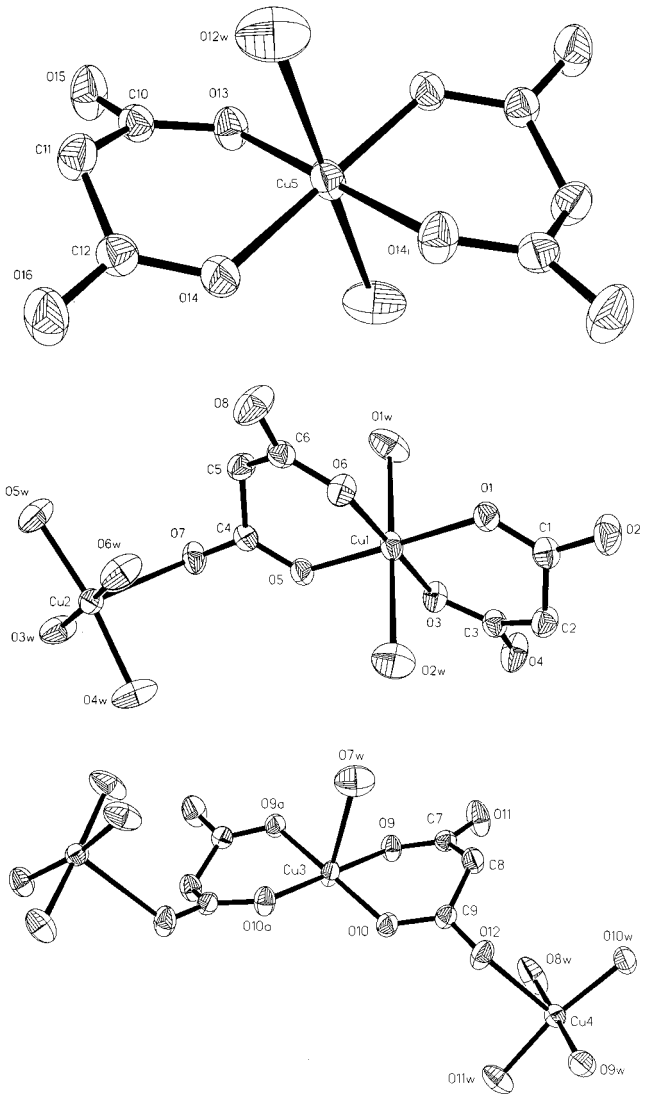

Figure 3. Perspective view of the mono- (a), di- (b), and trinuclear (c) copper(II) units of complex **2** along with the atom numbering. The thermal ellipsoids are drawn at the 30% probability level and the hydrogen atoms have been omitted for clarity.

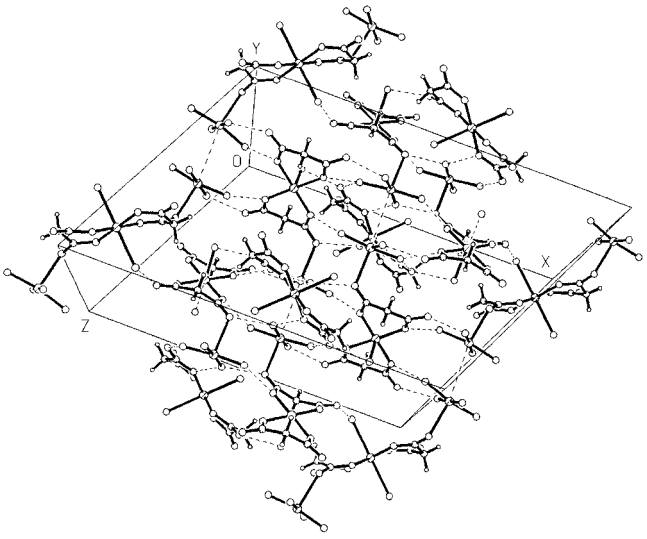

Figure 4. Contents of the unit cell of complex **2** showing the hydrogen bonds (broken lines) linking the mono-, di-, and trimeric units.

(41) Gleizes, A.; Julve, M.; Verdaguer, M.; Real, J. A.; Faus, J.; Solans, X. *J. Chem. Soc., Dalton Trans.* **1992**, 3209.
(42) Stiefel, E. I.; Brown, G. F. *Inorg. Chem.* **1972**, *11*, 434.

C(12)), which confirms the suggestion[43] that in malonato complexes in which there is a six-membered chelate ring, the planes of the two carboxylate groups are twisted more closely to the C−C−C− plane leading to a considerable opening of the expected tetrahedral angle.

The neutral dinuclear entity consists of a diaquabis(malonato)-copper(II) anion and a tetraaquacopper(II) cation connected through a carboxylato bridge exhibiting the *anti*−*syn* bridging mode. The crystallographically independent copper atoms, Cu(1) and Cu(2), exhibit different enviroments, distorted octahedral at Cu(1) and square pyramidal at Cu(2). The entire structure of this dimer is very close to that previously reported by Chattopadhyay et al.[28] for the same dimer as an isolated molecule. The practically identical values of the bond distances and angles, concerning the Cu(1)O(5)C(4)O(7)Cu(2) bridging skeleton in the two dimers, account for the very close intradimer copper−copper separation, 5.7393(11) Å (this work) versus 5.78 Å.[28]

The structure of the trinuclear $\{[Cu(H_2O)_4]_2[Cu(mal)_2(H_2O)]\}^{2+}$ cation is formed by a central aquabis(malonato)-copper(II) entity that is linked to two peripheral tetraaquacopper-(II) units through carboxylato bridges which exhibit the *anti*−*syn* configuration. A mirror plane, that contains the Cu(3)−O(7w) bond, bisects the trimer in two equivalent halves. The coordination around the two crystallographically independent copper atoms (Cu(3) and Cu(4)) is distorted square pyramidal. Four coplanar carboxylate oxygen atoms from two malonato ligands with nearly identical bond lengths (1.938(4) and 1.941-(2) Å for Cu(3)−O(9) and Cu(3)−O(1O), respectively) build the basal plane around Cu(3), whereas a weakly coordinated water molecule (2.508(3) Å for Cu(3)−O(7w)) occupies the axial position. Cu(3) lies in the basal plane, with all of its bond angles nearing 90°. At Cu(4), four coplanar oxygen atoms from four water molecules are located at the corners of an almost perfect square, with the copper to oxygen bond lengths varying in the 1.915(2)−1.936(2) Å range, whereas a malonato-oxygen (O(12)) occupies the axial position at a somewhat longer distance (2.381(3) Å for Cu(4)−O(12)). Cu(4) is displaced by 0.1158(5) Å from its basal plane toward O(12). The intratrimer Cu(3)···Cu(4) separation is 5.857(2) Å, a value which agrees well with that observed in the preceding dinuclear unit, in which the same carboxylate bridging pathway occurs.

Infrared Spectra. The IR spectra of complexes **1**−**3** have significant differences, particularly in the regions of the stretching and bending frequencies of their carboxylate groups. Two strong peaks at 1700 (ν_{as}(OCO)) and 1400 cm^{-1} (ν_s(OCO)) are observed in the infrared spectrum of uncoordinated malonate.[44,45] In addition, medium intensity peaks at 800 and 750 cm^{-1} are assigned to the OCO bending frequencies.[45] These frequencies are significantly shifted to lower frequencies by the coordination of malonate to metal ions, and in the present case, the chelating and/or bridging role of the malonate ligand can be easily detected. The infrared spetrum of complex **2** is the most interesting one in the series because of the coexistence of three different molecules where bidentate malonate (mononuclear unit), bidentate, and anti−syn bridging malonate (di- and trinuclear entities) occur. So, it deserves to be outlined that the ν_{as}(OCO absorptions appear at 1589 and 1541 cm^{-1} in **1** and at 1642 and 1569 cm^{-1} in **3**, whereas they are located at 1670, 1642, 1589, and 1569 cm^{-1} in **2**. Regarding the ν_s(OCO) features, they are centered at 1448 and 1363 cm^{-1} (**1**); 1458 and 1392 cm^{-1} (**3**); and at 1458, 1443, 1392, and 1378 cm^{-1} (**2**). Finally, the δ(OCO) absorptions are located at 797 and 745 cm^{-1} (**1**); 812 and 745 cm^{-1} (**3**); and 812, 745, and 738 cm^{-1} (**2**). The greater structural variety of **2**, in comparison with the structures of **1** and **3**, accounts for the higher complexity of its IR pattern.

Synthetic Aspects of Malonate-Containing Copper(II) Complexes. Four crystal structures of copper(II) complexes that contain only malonate and water as ligands are known, their formulas being $\{[Cu(H_2O)_3][Cu(mal)_2(H_2O)]\}_n$ (**1**), $\{[Cu(H_2O)_4]_2[Cu(mal)_2(H_2O)]\}[Cu(mal)_2(H_2O)_2]$ $\{[Cu(H_2O)_4][Cu(mal)_2(H_2O)_2]\}$ (**2**), $\{[Cu(H_2O)_4][Cu(mal)_2(H_2O)]\}$ (**3**), and $[Cu(H_2O)_6][Cu(mal)_2(H_2O)_2]$ (**4**). The former two are the subject of the present work, whereas the structures of **3**[28] and **4**[26] were reported elsewhere. The structure of the $[Cu(mal)_2]^{2-}$ anion as either a sodium[45] or alkaline-earth salt is also known.[30] Previous studies of complex formation in aqueous solution between malonic acid and Cu(II) as a function of pH revealed the stepwise formation of the species $[Cu(Hmal)]^+$, [Cu(mal)], and $[Cu(mal)_2]^{2-}$.[46] In our synthetic work, we observed that the isolated dimer **3** is obtained from highly concentrated, hot solutions containing basic carbonate with an excess of malonic acid. The ionic salt **4** is formed by the slow evaporation of diluted aqueous solutions containing basic carbonate and malonic acid in a 1:1 molar ration. The final pH of these solutions must be kept at ∼3, through the careful addition of a poorly coordinating base. At higher pH values (obtained by further addition of NaOH or Na_2CO_3), the concentration in solution of $[Cu(mal)_2]^{2-}$ becomes significative, and the precipitation of $Na_2[Cu(mal)_2]$ takes place.[45] If the concentration of Cu(II) exceeds that of malonate, then mixed basic copper(II) salts are obtained. The use of complexing but less-basic bases, such as pyridine (in the case of **1**) and 4,4′-bipyridine (in the case of **2**), allowed us to obtain **1** and **2** by a smooth increase in the pH without the precipitation of undesired basic salts. It has been observed that the addition of pyridine[47] and other bases[48] causes the formation of a mixed-ligand complex [CuL(mal)] that avoids the formation of basic copper(II) salts, minimizes the concentration of free Cu(II), and because the pH is increased, favors the formation of $[Cu(mal)_2]^{2-}$. This seems to allow the slow growth of complexes **1** and **2**, instead of the dimers **3** and **4**. In summary, parameters such as pH, Cu(II):H_2mal molar ratio, total concentration, and temperature are very critical when attempting to prepare malonate-containing copper(II) complexes and compounds with closely associated formulas. However, the data shown in the present work illustrate that good results can be obtained by monitoring these parameters carefully.

Magnetic Properties of 1−3. The magnetic properties of **1** under the form of the $\chi_M T$ product versus T (χ_M being the magnetic susceptibility per two copper(II) ions) is shown in Figure 5. $\chi_M T$ at 290 K is equal to 0.80 cm^3 mol^{-1} K, a value that is as expected for two magnetically isolated spin doublets. This value remains practically constant throughout cooling from room temperature to 70 K, and it increases sharply at lower temperatures to attain a value of 2.73 cm^3 mol^{-1} K at 1.9 K. This curve reveals the occurrence of an overall ferromagnetic coupling in **1**. Upon examining the structure of this compound (Figure 1), one sees that two different *anti*−*syn* carboxylato

(43) Karipides, A.; Ault, J.; Reed, A. T. *Inorg. Chem.* **1977**, *11*, 3299.
(44) Subramaniam, P. S.; Dave, P. C., Boricha, V. P.; Srinivas, D. *Polyhedron* **1998**, *17*, 443.
(45) Schmelz, M. J.; Nagakawa, I.; Mizushima, S.; Quagliano, J. V. *Inorg. Chem.* **1959**, *81*, 287.
(46) Smith, R. M.; Martell, A. E. *Critical Stability Constants*; Plenum Press: New York, 1975; Vol. 2, p 165. Smith, R. M.; Martell, A. E. *Critical Stability Constants*; Plenum Press: New York, 1982; Vol. 5, p 308.
(47) Mihailova, V.; Bonnet, M. *Bull. Soc. Chim. Fr.* **1969**, *12*, 4258.
(48) Bonnet, M., Paris, R. A. *Bull. Soc. Chim. Fr.* **1966**, 747.

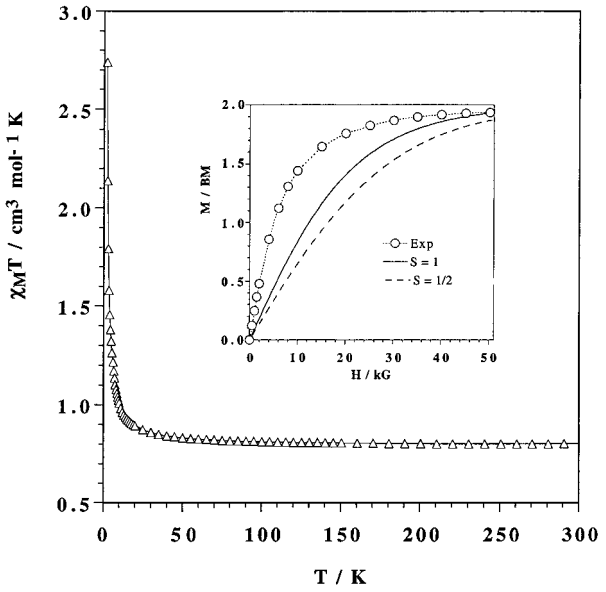

Figure 5. Thermal dependence of the $\chi_M T$ product for complex **1**: (△) experimental data; (—) best fit trough eq 1. The inset shows the magnetization vs the applied magnetic field at 2.0 K: (○) experimental data; (- - -) Brillouin function for two magnetically noninteracting spin doublets; (—) Brillouin function for a spin triplet.

bridges alternate regularly within the chain. Consequently, the alternating intrachain magnetic interactions are denoted J and j. A priori, two different situations can be envisaged: alternating either ferro- or ferro-antiferromagnetic magnetic interactions. In the latter case, the ferromagnetic interaction must be stronger than the antiferromagnetic one. The appropriate Hamiltonian to model the magnetic behavior of **1** is given by eq 1

$$\hat{H} = -J\sum_i[\hat{S}_{2i}\cdot\hat{S}_{2i-1} + \alpha\hat{S}_{2i}\cdot\hat{S}_{2i+1}] \qquad (1)$$

where α is the alternation parameter and αJ is equal to j. A numerically exptrapolated expression, based on rings of increasing size that contain only spin doublets (the calculations were limited up to 14 spin rings)[49] allowed us to successfully match the magnetic data. The best fit parameters are $J = 3.0$ cm^{-1}, $j = 1.9$ cm^{-1}, $g = 2.05$, and $R = 1.2 \times 10^{-4}$. The variable R is the agreement factor, defined as $\sum_i [(\chi_M T)_{obs}(i) - (\chi_M T)_{calc}(i)]^2/\sum[(\chi_M T)_{obs}(i)]^2)$. All of our attempts to model its magnetic behavior, with J and j of different sign, failed. The magnetization curve of **1** as a function of the applied field at 2 K (see inset of Figure 5) sharply increases with the applied field, attaining a saturation value of $\sim 2\ \mu_B$ (as expected for two spin doublets with a g value close to 2.0).The magnetization data lie well above those of the Brillouin functions for a spin triplet (ferromagnetic dimer) and two magnetically isolated spin doublets. This is in agreement with the spin correlation occurring in a ferromagnetically coupled chain, thus supporting the occurrence of intrachain ferromagnetic interactions in **1**.

Regarding the intrachain ferromagnetic couplings observed in **1**, two topics warrant mentioning: (i) their weak magnitude and ferromagnetic nature and (ii) the possibility of establishing which of the two carboxylato bridges is responsible for the stronger coupling. Concerning the first topic, weak antiferro- or ferromagnetic interactions are observed in carboxylato-bridged copper(II) complexes in which the carboxylato adopts the *anti*−*syn* conformation.[13−21] The small overlap between the magnetic orbitals of the copper atom through the *anti*−*syn* carboxylato bridge, for a Cu−O−C−O−Cu skeleton that is planar,[13,16] accounts for the weak antiferromagnetic coupling observed. This overlap is significantly reduced for cases in which the Cu−O−C−O−Cu skeleton deviates from the planarity (out-of-plane exchange pathway), thus reducing the antiferromagnetic contribution, and the ferromagnetic term becomes dominant.[18,21] In the case of **1**, the relative orientation of the metal-centered magnetic orbitals within the chain is depicted in Scheme 2.

Scheme 2

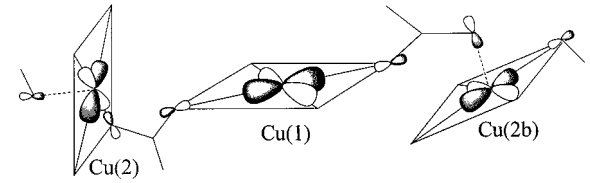

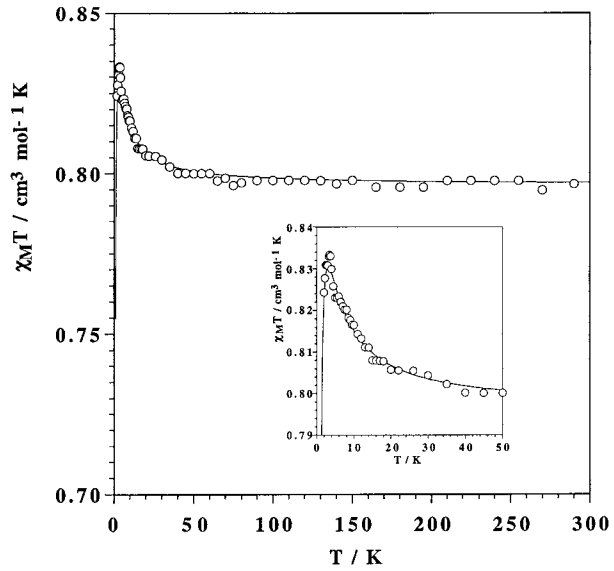

Figure 6. Thermal dependence of the $\chi_M T$ product for the dinuclear complex **3**: (○) experimental data; (—) best fit trough eq 2. The inset shows the low-temperature region.

The magnetic orbital at each copper atom is defined by the short equatorial bonds, and it is of the $d_{x^2-y^2}$ type with possibly some mixture of the d_{z^2} character in the axial position. There it can be seen that the out-of-plane exchange pathway is involved in the Cu(1)−O(5)-C(6)−O(7)−Cu(2) and Cu(1)−O(1)-C(1)−O(2)−Cu(2b) fragments. Consequently, ferromagnetic couplings would be predicted, as observed. Concerning the second topic, the fact that the O(5)−C(5)−O(5) plane and the equatorial plane at Cu(2) ((O(2w)O(4w)O(3w)O(7)) are nearly orthogonal (dihedral angle of 94.4°), and this carboxylato bridge connect two equatorial bonds (Cu(1)−O(5) and Cu(2)−O(7)), clearly supports the assignation of the strongest ferromagnetic coupling ($J = 3.0$ cm^{-1}) to the Cu(1)···Cu(2) pair. The weakest coupling ($j = 1.9$ cm^{-1}) most likely corresponds to the Cu(1)−O(1)−C(1)−O(2)−Cu(2b) unit, in which the out-of-plane exchange pathway through the axial O(2) atom is operative, with the Cu(1)···Cu(2b) separation (4.640(1) Å) being somewhat longer than that of Cu(1)···Cu(2) (4.854(1) Å).

The magnetic properties of **3** are shown in Figure 6 (χ_M being the magnetic susceptibility per two copper(II) ions). This curve is typical a ferromagnetically copper(II) dimer with a weak intermolecular antiferromagnetic interactions (θ) and/or zero-field splitting (D). The analysis of the magnetic data by the

(49) Borrás-Almenar, J. J.; Coronado, E.; Curély, J.; Georges, R.; Gianduzzo, J. J. *Inorg. Chem.* **1994**, *33*, 5171.

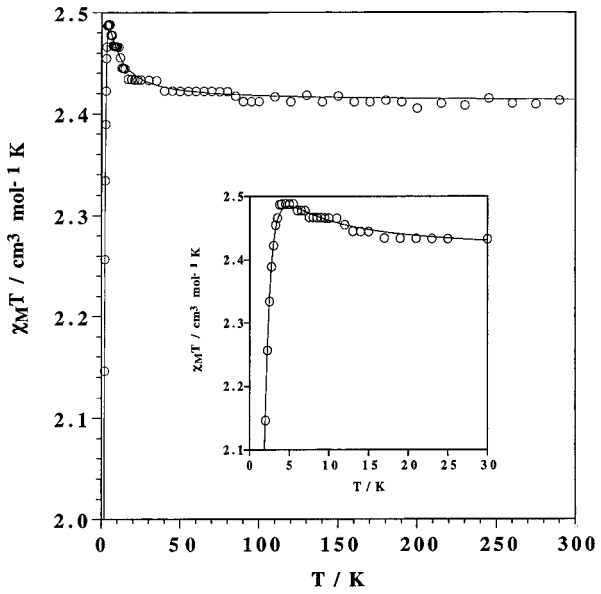

Figure 7. Thermal dependence of the $\chi_M T$ product for complex **2**: (o) experimental data; (–) best fit trough eq 4. The inset shows the low-temperature region.

appropriate expression through the Hamiltonian (eq 2)[50]

$$\hat{H} = -J\hat{S}_A \cdot \hat{S}_B + g\beta(\hat{S}_A + \hat{S}_B)\,\mathrm{H} + \hat{S}_A D\hat{S}_B \qquad (2)$$

where J is the intradimer magnetic coupling, $S_A = S_B = 1/2$ (local spins) and $g = g_A = g_B$ (Landé factors). The best fit parameters are $J = +1.8$ cm^{-1}, $g = 2.06$, $D = -0.3$ cm^{-1}, $\theta = -0.36$, K and $R = 1.2 \times 10^{-4}$. The weak intradimer ferromagnetic coupling observed in **3** is in agreement with the out-of-plane Cu(1)−O(1)−C(16)−O(10)−Cu(2) bridging skeleton (*anti*−*syn* carboxylato conformation) that is operative in this compound; the equatorial Cu(1)−O(11) (1.948(3) Å) and axial Cu(2)−O(110) (2.393(4) Å) bonds are involved in the exchange pathway. This situation is very similar to that found in the Cu(1)−O(1)−C(1)−O(2)−Cu(2b) fragment from **1**. It is very satisfying to note that the ferromagnetic coupling in both cases is nearly identical, the slightly smaller value in **3** being due to the somewhat longer axial bond in this case (2.393(4) Å in **3** against 2.185(2) Å in **1**).

The magnetic behavior of compound **2** is shown in Figure 7, under the form of a $\chi_M T$ versus T plot (χ_M being the magnetic succeptibility for six copper(II) ions). At 290 K, $\chi_M T$ is equal to 2.42 cm^3 mol^{-1} K, a value that is as expected for six magnetically isolated spin doublets. This value remains constant during cooling from room temperature to 50 K, and it increases smoothly at lower temperatures, reaching a maximum value of ∼2.49 cm^3 mol^{-1} K at 5.0 K. Then, the $\chi_M T$ decreases abruptly (see inset of Figure 7), and it attains a value of 2.14 cm^3 mol^{-1} K at 1.9 K. This curve is typical of an overall weak ferromagnetic coupling with antiferromagnetic interactions in the very low temperature range. The structural complexity of **2** (coexistence of mono-, di-, and trinuclear units) makes the theoretical analysis of its magnetic behavior very difficult. In addition to the presence of antiferromagnetic intermolecular interactions, the occurrence of two magnetic interactions, one within the dimer and the other within the trimer, which can be both ferromagnetic or of a different sign (the ferromagnetic coupling being stronger than the antiferromagnetic one) account for this difficulty. However, the fact that the structure of the dimeric unit that is present in **2** is practically the same as that of compound **3**[28] simplifies the analysis of the magnetic properties of **2**. This is why we have synthesized complex **3** and investigated its magnetic properties. The magnetic coupling observed in **3** has been introduced as a fixed parameter in the magnetic analysis of **2**, thus avoiding the overparametrization.

The total magnetic susceptibility of **2** (χ_{Mtot}) is given by the sum of the contributions of the mono-, di-, and trinuclear units (eq 3)

$$\chi_{Mtot} = \chi_{Mmon} + \chi_{Mdim} + \chi_{Mtrim} \qquad (3)$$

The first term is the Curie law for a mononuclear Cu(II) complex ($\chi_{M\ mon} = N\beta^2 g_{mon}^2/4kT$), the second term is constant (the magnetic parameters being those of **3**, eq 2), and the third is derived through the Hamiltonian eq 4

$$\hat{H} = -J(\hat{S}_{Cu3} \cdot \hat{S}_{Cu4} + \hat{S}_{Cu3} \cdot \hat{S}_{Cu4a}) + \sum_{i=1}^{3} g_{Cui}\beta\hat{S}_{Cui}\mathbf{H} \qquad (4)$$

where J describes the magnetic coupling between adjacent copper(II) ions and $S_{Cui} = 1/2$ (local spins). In an attempt to avoid overparametrization, the magnetic coupling between the terminal copper(II) ions within the trimer was neglected, and only one g value was considered ($g_{mon} = g_{Cui} = g$). To take into account the intermolecular interactions, a molecular-field correction term (θ) was added to the susceptibility expression of the trimer (see Table 4 and Figure 4, which shows the hydrogen bonding interactions that connect the trimeric unit with the mono- and dimeric ones). Least-squares fit to the data of **2** lead to $J = +1.2$ cm^{-1}, $g = 2.07$, $\theta = -0.4$ K, and $R = 2.2 \times 10^{-4}$. The theoretical curve matches the data shown in Figure 7 very well. Once more, a weak ferromagnetic coupling through the *anti*−*syn* carboxylato bridge is observed. An inspection of the structure of the trinuclear unit in **2** shows that the out-of-plane exchange pathway is between the central and the terminal copper(II) ions. The value of the magnetic coupling is quite close to those observed in the similar copper(II) pairs of **1** (1.9 cm^{-1}) and **3** (1.8 cm^{-1}).

Conclusion

In conclusion, three main points emerge from the present work: First, there is a great structural diversity among the malonato-containing copper(II) complexes, which is exemplified by the structures of the complexes **1**−**4**. Second, there is a need for detailed structural information that would facilitate the correct interpretation of the magnetic properties in apparently simple systems. Third, the dicarboxylate malonate is a very versatile ligand that allows the preparation of both discrete and extended systems which are able to mediate significant ferromagnetic interactions between copper(II) ions bridged by *anti*−*syn* carboxylate groups.

Acknowledgment. The financial support provided by the Spanish Dirección General de Investigación Científica y Técnica (DGICYT), through Projects PB97-1479-C02-02 and PB97-1397, and the European Union (TMR Program), through Contract ERBFM-RXCT980181, is gratefully acknowledged.

Supporting Information Available: X-ray crystallographic files for complexes **1** and **2** in CIF format. This material is available free of charge via the Internet at http://pubs.acs.org.

(50) Kahn. O. *Molecular Magnetism*; VCH: New York, 1993; p 137.

IC9908165